Department of Defense
Legacy Resource Management Program

PROJECT 17-834

An Early-Warning Mapping Tool for Forecasting Fire Risk on DoD Lands in the Arid West

Miranda E. Gray, CSP
Luke J. Zachmann, CSP
Brett G. Dickson, CSP
Josh Gage, Gage Cartographics

September 2018

Project No: 17-834
Title: An early-warning mapping tool for forecasting fire risk on DoD lands in the arid West
Deliverable: Metadata and summary of methods used to develop web application features

Study Area

Environmental Protection Agency (EPA) level III desert ecoregions were used to delineate the bounds of statistical models and maps of large fire probability. The different climates, topography, dominant vegetation, and vegetation productivity across these deserts influence fuels and fire behavior, and contribute to different drivers of fire risk (Abatzoglou and Kolden 2011, Brooks and Chambers 2011). The Snake River Plain is considerably lower, more gently sloping, and contains more grassland vegetation types than the Basin and Range to the south. The Northern and Central Basin and Range are cold desert shrublands and, relative to the warm desert shrublands, are characterized by higher precipitation and vegetation productivity. In contrast, warm desert shrublands characterize most of the Mojave and Sonoran Deserts in the southern most extent of the study area, where precipitation is relatively low and native vegetation types exhibit generally low productivity (see https://www.epa.gov/eco-research/level-iii-and-iv-ecoregions-continental-united-states).

Model Design

Using historical fire observations across the desert ecoregions, we modeled the conditional probability of large fire (i.e., > 300 acres), which we define as the probability that an area on the landscape will burn in a large fire following either an ignition event or fire spread to that area (e.g., see Gray et al., 2018). We chose to use 300 acres because this threshold accounted for at least 97 percent of the total area burned from

1992-2016, in all ecoregions except for the Sonoran Desert, where this threshold was only 50 acres (Short 2017). Because the minimum detectable fire size of our large fire dataset was 300 acres (see below), we also used a 300-acre threshold for the Sonoran. We used the random forest (RF) classification algorithm to train predictive models of large fire probability. Random forest is a machine learning technique that recursively partitions variables to classify an outcome of interest, in this case small or large fire events (Prasad et al. 2006). Given the broad-scale differences described above in the drivers of fire risk across desert ecoregions, we trained RF models separately for each of three desert sub regions, namely, the Snake River Plain (Model 1), the Northern and Central Basin and Range (Model 2), and the Mojave and Sonoran Deserts (Model 3; Fig. 1).

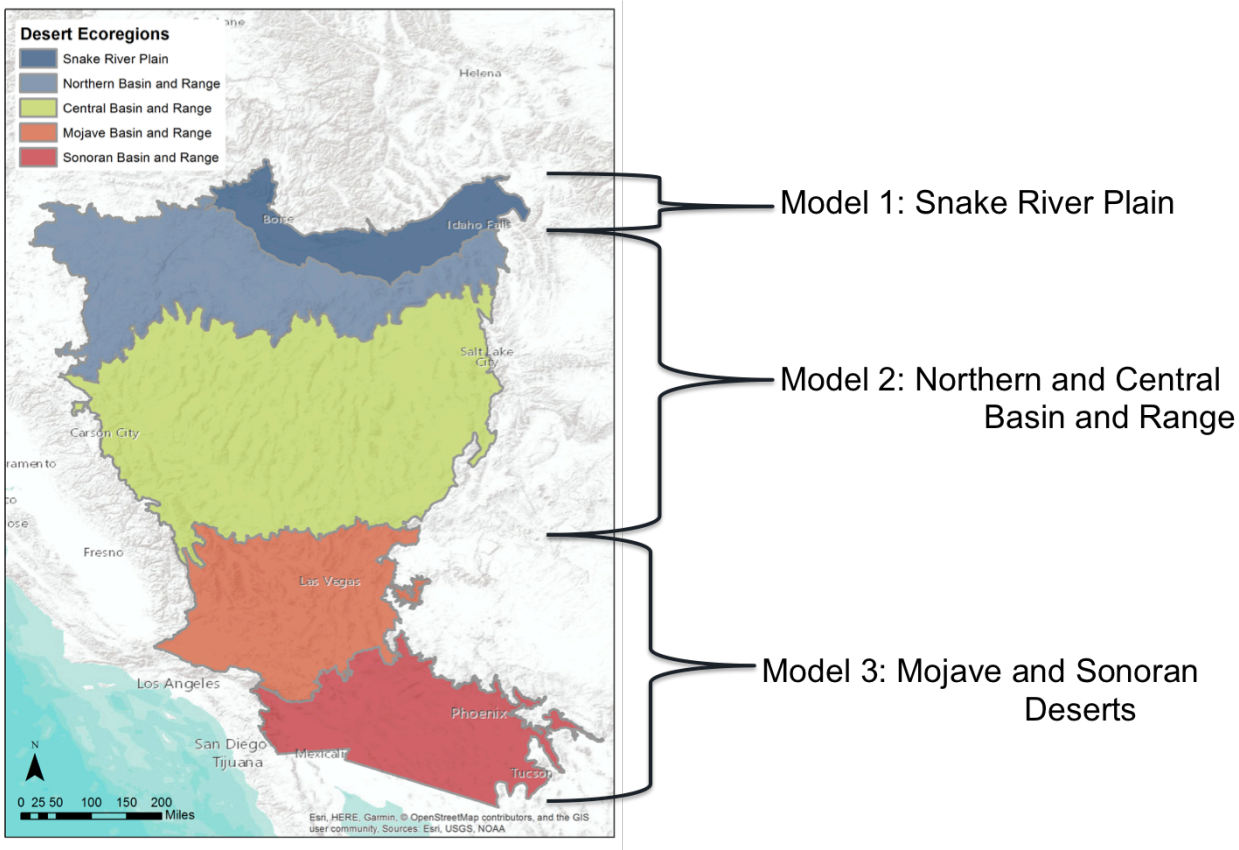

Figure 1. The Random Forest (RF) classification algorithm, which is a machine learning technique, was used to train models of large fire probability separately for three desert sub regions.

Response Variables

The binary response variable in our RF models was a point on the landscape where there was an ignition event that resulted in a small fire (i.e., < 300 ac; "0" response) or that historically burned in a large fire (i.e., > 300 ac; "1" response). Following methods of Gray et al. (Gray et al. 2018) samples of large fires that occurred from 2005-2018 were drawn from the MODerate-resolution Imaging Spectroradiometer (MODIS) Burned Area (BA) dataset (Roy et al. 2008), which is a global, monthly 500-m gridded product that contains calendar day-of-burn and quality information. Large fire samples were taken as the centroid of 500-m pixels. To avoid spatial autocorrelation of predictor variables (see below) within large fires, we drew at most one sample (a point location) from within each large fire. As mentioned above, the minimum detectable burn size of the BA dataset is 300 acres (Giglio et al. 2009, Roy and Boschetti 2009), and thus samples of small fires were drawn from a well-vetted, point-of-occurrence database of reported fires in the United States from 2005-2016 that contains day-of-discovery (Short 2017). We matched these small fire samples with an equal sized random sample of small fires, within each desert sub region. This ensured a balanced, 1:1 ratio of large to small fires with which to train RF models.

While spatial autocorrelation of predictor variables is invariably present within individual fires, burning conditions can also be quite heterogeneous over the course of a single large fire (Turner 2010). Therefore, we took a further step to capture this heterogeneity. We repeated the above sampling and model building protocol using 10 different random samples of large and small fires, such that each of 10 RF models were not entirely independent but contributed slightly novel information to a mean prediction across those 10 models. This type of ensemble modeling provides a means of producing models that are more accurate than the individual models that make them up, while depicting the variance across predictions, which helps users better assess risk (Dietterich 2000, Palmer et al. 2005).

Predictor Variables

Predictor variables were derived to describe the fuels, topography, climate, and fire weather preceding fire (Table 1). Specifically, an individual large or small fire sample was spatially related to long-term predictors derived over a multi-year period and near-term predictors derived over the weeks and months preceding fire occurrence. The integration of predictors in this way resolves the dynamic probability of large fire into long-term drivers of fire, and near-term land surface and ambient conditions directly leading up to a fire event. To account for the difference in spatial scales between a large fire and the native resolution of spatial predictors (i.e., ranging from 30 m to 4 km), we used a moving window to summarize predictors within a circular kernel with radius 630 m. Predictor variables that were not in a native 250-m resolution were resampled using bilinear interpolation.

1. Fuel and Topography Variables

To characterize long-term live fuel availability, we used the Enhanced Vegetation Index (EVI, 250-m resolution) from the MODIS MOD13Q1 v006 product (Didan 2015), which provides a proxy for total vegetation. We used a multi-year time-series of EVI to capture the variability in overall biomass production, but also as a basis to capture variability in sub-pixel vegetation dynamics (e.g., Helman et al., 2015). MOD13Q1 are 16-day composites computed from atmospherically corrected, bi-directional daily surface reflectance. We only retained observations that were free of ice and snow. We extracted the following EVI metrics from 2000 (the year MODIS was deployed) to the approximate date of fire occurrence: (i) reflectance values representing maximum, minimum and selected percentile values (10, 25, 50, 75 and 90% percentiles); (ii) mean reflectance values for observations between selected percentiles (for the max-10%, 10-25%, 25-50%, 50-75%, 75-90%, and 90%-max); and (iii) slope of linear regression of EVI versus image date. We included these metrics to build a generic feature space to characterize vegetation over at least five complete years, as they have been used in

previous machine-learning applications to characterize regional-scale vegetation cover (Hansen et al. 2013).

We characterized the near-term live vegetation abundance and condition with EVI observations in the five months prior to fire occurrence. Preliminary analyses of pre-fire EVI in burned areas indicated that, on average, the five months leading up to fire captured the seasonal growth cycle of fuels available to burn. Therefore, we included the maximum and minimum of EVI in these five months. To account for senesced biomass from the year prior to fire occurrence (i.e., lag year) that can remain standing as fuel for a subsequent fire season (Gray et al. 2014), we included these same EVI metrics for the lag year. Lastly, to capture the seasonal fuel growth above or below the long-term background EVI, we subtracted the long-term 10^{th} percentile of EVI from the current 5-month maximum EVI, for both the current and lag year (e.g., Casady et al., 2013).

To characterize topographic variables, namely, elevation, slope, aspect, and terrain roughness (standard deviation of elevation), we used the Shuttle Radar Topography Mission digital elevation data (Farr et al., 2007; 30-m resolution).

2. Climate and Weather Variables

We incorporated climate predictors computed from monthly normals of temperature and precipitation for the period 1981-2010, as derived from the Parameter-elevation Regressions on Independent Slopes Model (PRISM Norm81m vM2; 800-m resolution; Daly et al., 1994). We selected five metrics that summarized long-term annual means, extremes, and seasonality of temperature and precipitation, and which have been used previously to capture the amount and dryness of biomass to predict fire occurrence (Krawchuk et al. 2009, Moritz et al. 2012). These metrics included annual precipitation, precipitation of the warmest month, mean temperature of the wettest month, mean temperature of the warmest month, and temperature seasonality (i.e., the standard deviation of mean monthly temperatures; O'Donnell and Ignizio, 2012).

Standard meteorological variables known to influence the daily fire and fuel environment were taken from the GRIDMET gridded daily surface meteorological dataset (4-km resolution; Abatzoglou, 2013). We incorporated the total precipitation, mean minimum and maximum temperature, mean minimum and maximum relative humidity, and mean wind speed and direction, for the week preceding fire occurrence. Standard weather variables have also been compiled into indices that more directly address the processes by which they influence fire behavior and fuels, including the Energy Release Component (ERC), the Burning Index (BI), and 100- and 1000-hr dead fuel moistures (fm100 and fm1000). These indices are components of the US National Fire Danger Rating System (NFDRS) and are derived from models built on the combustion physics and moisture dynamics of the fuel environment, here assuming a consistent fuel model 'G' typified by short needle pine and heavy dead loads (Schlobohm and Brain 2002, Abatzoglou 2013). The fm100 and fm1000 indices represent the modeled moisture content of large dead fuels in the 1 to 3 inch diameter class and the 3 to 8 inch diameter class, respectively. ERC is a cumulative fuel moisture index reflecting the contribution of all live and dead fuel moistures on the potential heat release, and is also an input into the BI, which additionally incorporates the potential rate of fire spread. GRIDMET assumes that the persistent fuel environment includes all size classes of dead fuels, as well as herbaceous and woody live fuels, and all contribute to the derived values of these indices. We incorporated the mean values of ERC, BI, fm100, and fm1000 in the week preceding fire occurrence.

Table 1. Spatially Explicit climate, weather, fuel, and topography predictors of large fire probability, including the data source and spatial resolution.

Predictor Set	Source	Resolution
Long-term climate variables	PRISM[1]	800 m
Annual precipitation, temperature seasonality (CV), precipitation of the warmest month, mean temperature of the wettest month, mean temperature of the warmest month		
Long-term land surface variables		
EVi percentiles and interval means preceding fire year		

Elevation, slope, aspect, topographic roughness	MODIS USGS	250 m 30 m
Near-term land surface variables		
EVI[2] minimum, maximum, and change from background EVI in the five months preceding fire	MODIS USGS	250 m 30 m
Near-term weather variables 100- and 1000-hr fuel moisture, burning Index, precipitation, temperature, relative humidity, specific humidity, potential evapotranspiration, solar radiation, wind speed, wind direction, Palmer Drought Severity Index	GridMet[3]	4 km

[1] PRISM = Precipitation-elevation Regressions on Independent Slopes Model

[2] EVI = Enhanced Vegetation Index, an index of fuel availability that is derived from 16-day composites of MODIS imagery.

[3]GridMet = Gridded Surface Meteorological Data. Values were taken for the week preceding fire occurrence.

Mapped Products

Using 10 trained RF models, we derived spatially explicit predictions of the mean and standard deviation of large fire probability at a 250-m resolution. The extent of mapped predictions was limited to all USGS HUC8 watersheds that intersected DoD installations within the desert ecoregions (U.S. Geological Survey and U.S. Department of Agriculture Natural Resources Conservation Service 2013). Agricultural land cover (i.e., cultivated crops) from the National Land Cover Dataset (Homer et al., 2015), urban areas from the US Census Bureau (available at https://www.census.gov/geo/maps-data/data/cbf/cbf_ua.html), and waterbodies from the USGS National Hydrography Dataset (available at https://www.usgs.gov/core-science-systems/ngp/national-hydrography/access-national-hydrography-products) were masked from the final extent.

Models were trained and predictions implemented within Google Earth Engine (GEE; Gorelick et al., 2016), which is a cloud-based platform that makes terabyte-scale analysis available on an extensive catalog of satellite imagery and geospatial datasets.

Daily spatial predictions were created at one-week intervals from 2005 through the present. To create predictions for the present week, we developed a continuous integration (CI) 'pipeline' to generate new predictions as soon as the dynamic predictors upon which the model is conditioned become available in GEE. The refresh rate of each predictor can vary, according to the data sources. For example, GRIDMET assets are updated approximately every two days, whereas the MODIS EVI products are updated approximately every eight days. The pipeline, which tests for the availability of predictors against the requirements of the model, runs on a schedule — compiling each Monday morning at 04:00 Pacific Standard Time. If all of the criteria are met, a new prediction is generated, appended to the existing collection, and pushed up to the interactive mapping tool.

Dataset Evaluation

We used the MODIS BA and FOD datasets to generate a sample from within all large fires from 2005-2018, and an equal-sized random sample of small fires from 2005-2016, to evaluate the model on a testing dataset (n = 61, 328, and 136 for Models 1, 2, and 3, respectively). These samples were 'seeded' with a random number generator different from any of the training samples, and so this testing dataset can be considered partially independent from the training datasets. Again, large fire samples were taken as the centroid of 500-m pixels. Using predictions (i.e., raster maps) of large fire probability from 2005 through 2018, we extracted predicted values at the time (i.e., the closest prediction in time prior to fire occurrence) and location of individual testing points. Based on this training data, overall accuracy of the models ranged from 77% to 90% (Table 2).

We extracted variable importance values using the 'rfpimp' package in Python (available at https://github.com/parrt/random-forest-importances). We ranked predictor variable importance based on the permutation importance, which directly measures importance by observing the effect on model accuracy by randomly permuting the values of each predictor variable (Cutler et al. 2007). Since RF 'spreads'

variable importance across collinear variables, we used a built-in function in the 'rfpimp' package to permute collinear variables together and determine their relative, collective importance (Fig. 2).

Table 2. Confusion matrix based on a partially independent testing dataset of large and small fires samples from 2005-2018. Model predictions are the mean values across 10 Random Forest models in each of three desert subregions. False Negatives (FN) and False Positives (FP) were those testing samples incorrectly predicted as either a Large (FP) or Small (FN) fire.

	Reference		
Model 1 Prediction	Small	Large	Accuracy
Small	26	11 (FN)	
Large	3 (FP)	21	77%
Model 2 Prediction			
Small	134	34 (FN)	
Large	41 (FP)	119	77%
Model 3 Prediction			
Small	59	6 (FN)	
Large	7 (FP)	64	90%

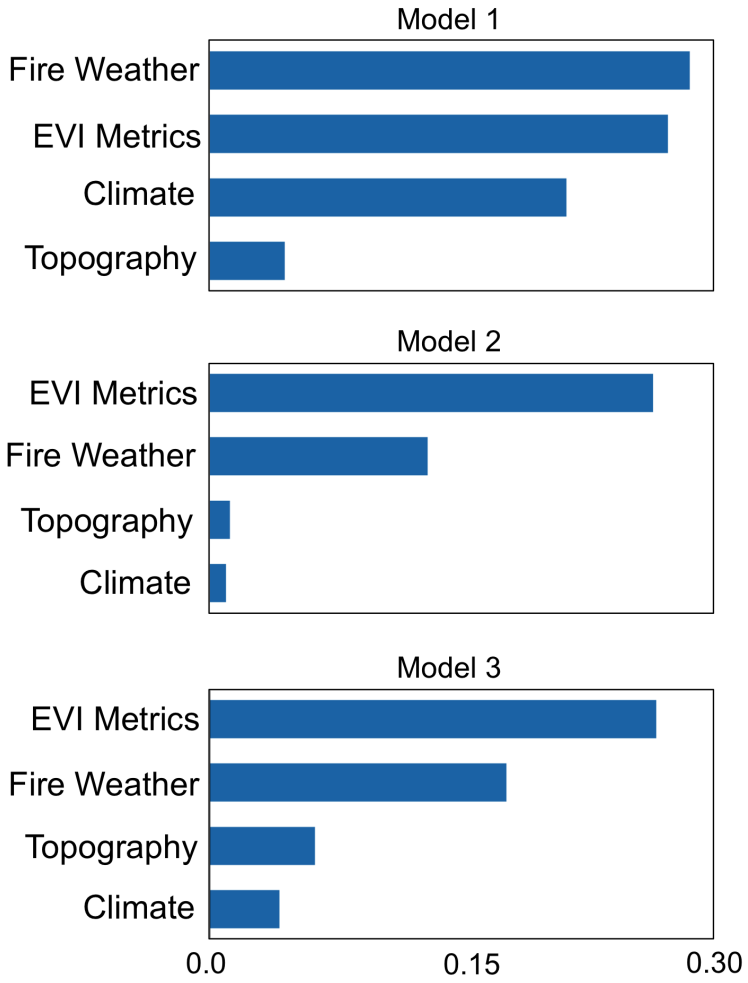

Figure 2. Relative variable importance for groups of predictors used to model large fire probability across three desert sub regions. Variable importance was determined by observing the effect on model accuracy by randomly permuting the values of each predictor variable.

References

Abatzoglou, J. T. 2013. Development of gridded surface meteorological data for ecological applications and modelling. International Journal of Climatology 33:121–131.

Abatzoglou, J. T., and C. A. Kolden. 2011. Climate change in western US deserts : potential for increased wildfire and invasive annual grasses. Rangeland Ecology & Management 64:471–478.

Brooks, M. L., and J. C. Chambers. 2011. Fire and invasive plants special feature: Resistance to invasion and resilience to fire in desert shrublands of North America. Rangeland Ecology & Management 64:431–438.

Casady, G. M., W. J. van Leeuwen, and B. C. Reed. 2013. Estimating winter annual biomass in the Sonoran and Mojave Deserts with satellite- and ground-based observations. Remote Sensing 5:909–926.

Cutler, D. R., T. C. Edwards, K. H. Beard, A. Cutler, K. T. Hess, J. Gibson, and J. J. Lawler. 2007. Random Forests for Classification in Ecology. Ecology 88:2783–2792.

Daly, C., R. P. Neilson, and D. L. Phillips. 1994. A statistical–topographic model for mapping climatological precipitation over mountainous terrain.

Didan, K. 2015. MOD13Q1 MODIS/Terra Vegetation Indices 16-Day L3 Global 250m SIN Grid V006. NASA EOSDIS Land Processes DAAC.

Dietterich, T. G. 2000. Ensemble Methods in Machine Learning. Multiple Classifier Systems 1857:1–15.

Farr, T. G., P. A. Rosen, E. Caro, R. Crippen, R. Duren, S. Hensley, M. Kobrick,

M. Paller, E. Rodriguez, L. Roth, D. Seal, S. Shaffer, J. Shimada, J. Umland, M. Werner, M. Oskin, D. Burbank, and D. Alsdorf. 2007. The Shuttle Radar Topography Mission. Reviews of Geophysics 45.

Giglio, L., T. Loboda, D. P. Roy, B. Quayle, and C. O. Justice. 2009. An active-fire based burned area mapping algorithm for the MODIS sensor. Remote Sensing of Environment 113:408–420.

Gorelick, N., M. Hancher, M. Dixon, S. Ilyushchenko, D. Thau, and R. Moore. 2016. Google Earth Engine: Planetary-scale geospatial analysis for everyone. Remote Sensing of Environment.

Gray, M. E., B. G. Dickson, and L. J. Zachmann. 2014. Modeling and mapping dynamic variability in large fire probability in the lower Sonoran Desert of southwestern Arizona. International Journal of Wildland Fire 23:1108–1118.

Gray, M. E., L. J. Zachmann, and B. G. Dickson. 2018. A weekly, continually updated dataset of the probability of large wildfires across western US forests and woodlands. Earth System Science Data 1:1715–1727.

Hansen, M. C., P. V Potapov, R. Moore, M. Hancher, S. A. Turubanova, and A. Tyukavina. 2013. High-Resolution Global Maps of. Science 342:850–853.

Helman, D., I. M. Lensky, N. Tessler, and Y. Osem. 2015. A phenology-based method for monitoring woody and herbaceous vegetation in mediterranean forests from NDVI time series. Remote Sensing 7:12314–12335.

Homer, C., J. Dewitz, L. Yang, S. Jin, P. Danielson, G. Xian, J. Coulston, N. Herold, J. Wickham, K. Megown, and N. Herold. 2015. Completion of

the 2011 National Land Cover Database for the conterminous United States. Photogrammetric Engineering and Remote Sensing 81:345–354.

Krawchuk, M. A., M. A. Moritz, M. A. Parisien, J. Van Dorn, and K. Hayhoe. 2009. Global pyrogeography: The current and future distribution of wildfire. PLoS ONE 4.

Moritz, M. a., M.-A. Parisien, E. Batllori, M. a. Krawchuk, J. Van Dorn, D. J. Ganz, and K. Hayhoe. 2012. Climate change and disruptions to global fire activity. Ecosphere 3:art49.

O'Donnell, M. S., and D. A. Ignizio. 2012. Bioclimatic Predictors for Supporting Ecological Applications in the Conterminous United States. U.S Geological Survey Data Series 691:10.

Palmer, T. N., G. J. Shutts, R. Hagedorn, F. J. Doblas-Reyes, T. Jung, and M. Leutbecher. 2005. Representing Model Uncertainty in Weather and Climate Prediction. Annual Review of Earth and Planetary Sciences 33:163–193.

Prasad, A. M., L. R. Iverson, and A. Liaw. 2006. Newer classification and regression tree techniques: Bagging and random forests for ecological prediction. Ecosystems 9:181–199.

Roy, D. P., and L. Boschetti. 2009. Southern Africa validation of the MODIS, L3JRC, and GlobCarbon burned-area products. IEEE Transactions on Geoscience and Remote Sensing 47:1032–1044.

Roy, D. P., L. Boschetti, C. O. Justice, and J. Ju. 2008. The collection 5 MODIS burned area product - Global evaluation by comparison with the MODIS active fire product. Remote Sensing of Environment 112:3690–3707.

Schlobohm, P., and J. Brain. 2002. Gaining an understanding of the National Fire Danger Rating System. National Wildfire Coordinating Group.

Short, K. C. 2017. Spatial wildfire occurrence data for the United States, 1992-2015 [FPA_FOD_20170508]. 4th Edition. Fort Collins, CO: Forest Service Research Data Archive.

Turner, M. G. 2010. Disturbance and landscape dynamics in a changing world. Ecology 91:2833–2849.

U.S. Geological Survey, and U.S. Department of Agriculture Natural Resources Conservation Service. 2013. Federal Standards and Procedures for the National Watershed Boundary Dataset (WBD). U.S. Geological Survey Techniques and Methods 11–A3:63.